Coercivity Enhancement in Zr_2Co_{11}-Based Nanocrystalline Materials Due to Mo Addition

Wenyong Zhang[1,2], Shah R. Valloppilly[2], Xingzhong Li[2], Ralph Skomski[1,2], Jeffrey E. Shield[2,3], and David J. Sellmyer[1,2]

[1]Department of Physics and Astronomy, University of Nebraska, Lincoln, NE 68588 USA
[2]Nebraska Center for Materials and Nanoscience, University of Nebraska, Lincoln, NE 68588 USA
[3]Department of Mechanical and Materials Engineering, University of Nebraska, Lincoln, NE 68588 USA

The Mo-content dependence of structure and magnetic properties of $Zr_{16}Co_{78-x}Mo_xSi_3B_3$ ($x = 0, 2, 3, 4, 5$) nanocrystalline materials has been studied. The samples consist of hard-magnetic Zr_2Co_{11} and soft-magnetic Co phases. The substitution of Mo for Co restrains the formation of Co, raises the content of Zr_2Co_{11}, and increases the mean grain size of Zr_2Co_{11}. Therefore, the coercive force of the sample increases with x. A coercive force of 7.9 kOe, which is a highest value reported among Zr-Co alloys, was achieved for $x = 5$. The anisotropy field of Zr_2Co_{11} remains almost unchanged with increasing Mo content.

***Index Terms*—Coercive force, intermetallic, magnetic property, nanomaterials.**

I. Introduction

Zr-Co alloys have attracted much attention due to interesting properties such as superconductivity, high glass forming ability, and potential suitabilibity for permanent magnetism [1]–[3]. Recently, much work was focused on hard magnetism of Zr-Co alloys. Zr_2Co_{11} is a hard magnetic phase with the anisotropy field of 34 kOe [4]. Depending on the preparation process, its crystal structure may be rhombohedral or orthorhombic. Although the basic structure is denoted as Zr_2Co_{11}, a range of composition exists and it is often found that the stoichiometry corresponds to $ZrCo_{5.1}$ [5]. Our recent work shows that the coercive force of Zr_2Co_{11}-based nanocrystalline material was enhanced by the addition of Zr. The maximum coercive force of 2.7 kOe was obtained for nanocrystalline Zr_yCo_{100-y} ($y = 18$). It was reported that the magnetic polarization of Zr-Co alloys was increased to 11.6 kG after the introduction of 15 at% Fe [6]. It is known that the coercive force of a permanent magnet should be larger than half of saturation magnetization in order to improve energy product as much as possible. It is necessary to further increase the coercive force of Zr_2Co_{11}-based nanocrystalline materials. In general, the maximum coercive force of hard magnetic material is about one third of the anisotropy field. Thus the maximum coercive force of Zr_2Co_{11}-based nanocrystalline material might be improved to about 11 kOe. It was found that B addition obviously improved the coercive force of Zr_2Co_{11}-based nanocrystalline material [7]. The coercive force of Zr_2Co_{11}-based nanocrystalline material also was efficiently enhanced by the introduction of Mo [8].

In this work, the structure-property relationship of nanocrystalline $Zr_{16}Co_{78-x}Mo_xSi_3B_3$ has been analyzed. The crystal structure of Zr_2Co_{11} is rhombohedral. The anisotropy field of Zr_2Co_{11} for nanocrystalline $Zr_{16}Co_{78-x}Mo_xSi_3B_3$ is almost constant. Mo addition is helpful for the formation of Zr_2Co_{11}. The coercive force of the sample increases with x. The focus of this work is the origin of coercive force enhancement.

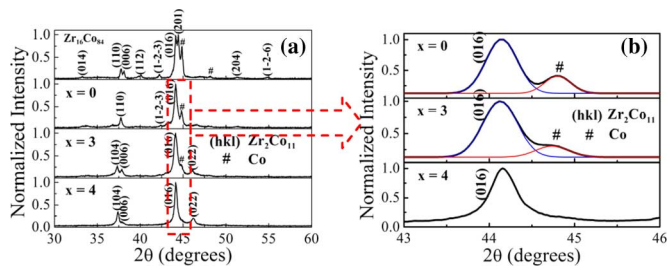

Fig. 1. XRD patterns of nanocrystalline $Zr_{16}Co_{84}$ and $Zr_{16}Co_{78-x}Mo_xSi_3B_3$ ($x = 0, 3, 4$).

II. Experimental Method

Ingots of $Zr_{16}Co_{84}$ and $Zr_{16}Co_{78-x}Mo_xSi_3B_3$ ($x = 0, 2, 3, 4, 5$) were arc melted from high-purity elements in an argon atmosphere. The ribbons were made by ejecting molten ingots in a quartz tube onto the surface of a rotating copper wheel with speeds of from 5 to 40 m/s. The typical size of ribbons is 2 mm wide and 50 μm thick. The phase identification was performed by Rigaku D/Max-B X-ray diffraction (XRD) with copper radiation. The magnetic properties were measured by superconducting quantum interference device (SQUID) magnetometer at fields up to 7T. The applied field is parallel to the long direction of ribbon.

III. Results and Disussions

Fig. 1 shows XRD patterns of nanocrystalline $Zr_{16}Co_{84}$ and $Zr_{16}Co_{78-x}Mo_xSi_3B_3$ ($x = 0, 3, 4$). The diffraction peaks of $Zr_{16}Co_{84}$ and $Zr_{16}Co_{78}Si_3B_3$ were indexed with rhombohedral Zr_2Co_{11} and hcp Co. The relative intensity of the diffraction peaks from Co for $Zr_{16}Co_{78}Si_3B_3$ are lower than that for $Zr_{16}Co_{84}$, indicating that combinational addition of Si and B evidently restrains the formation of Co. By the same token, Mo addition further inhibits the generation of Co. No diffraction peaks from Co or other phase were detected for $x = 4$, implying

Manuscript received March 02, 2012; accepted April 27, 2012. Date of current version October 19, 2012. Corresponding author: D. J. Sellmyer (e-mail: dsellmye@unlnotes.unl.edu).

Color versions of one or more of the figures in this paper are available online at http://ieeexplore.ieee.org.

Digital Object Identifier 10.1109/TMAG.2012.2198453

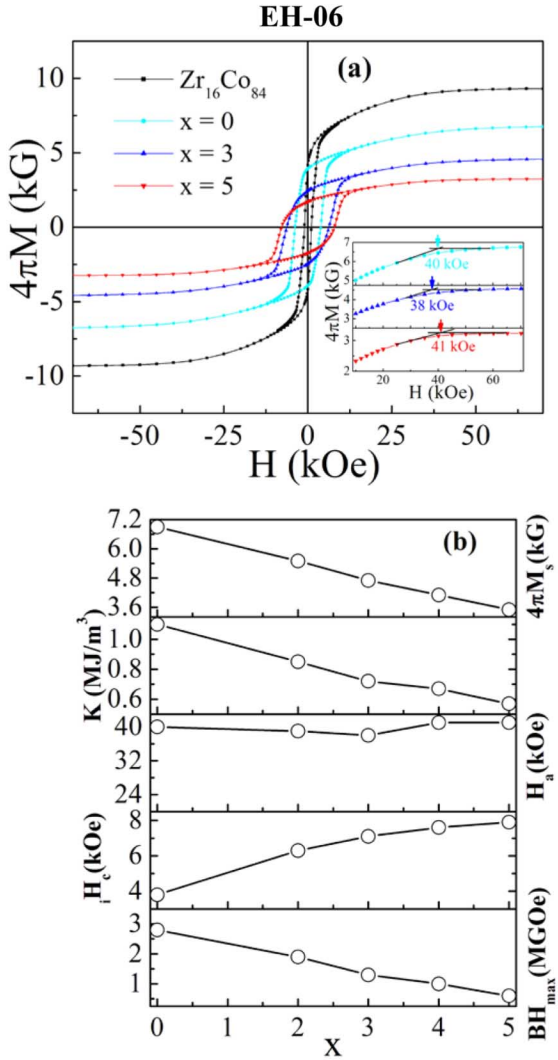

Fig. 2. Hysteresis loops of nanocrystalline $Zr_{16}Co_{84}$ and $Zr_{16}Co_{78-x}Mo_xSi_3B_3$ (x = 0, 3, 5) (the inset showing saturation fields for x = 0, 3, 5) (a) and deduced magnetic properties as a function of x (b).

predominantly single phase Zr_2Co_{11}. In addition, the full-width at half-maximum (FWHM) of diffraction peak at 44.12° for Zr_2Co_{11} is reduced with x. This means that the average grain size of Zr_2Co_{11} increases with x. FWHM of diffraction peak at 44.80° for Co increases with x. This indicates that the mean grain size of Co is reduced with x.

Fig. 2 presents the hysteresis loops of nanocrystalline $Zr_{16}Co_{84}$ and $Zr_{16}Co_{78-x}Mo_xSi_3B_3$ (x = 0, 3, 5) and the deduced magnetic properties as a function of x. It is seen that coercive force and magnetization of the specimen are strongly dependent on the alloy composition. The law of approach to saturation (LAS) is used to fit the high-field part of hysteresis loops [9]. The equation for LAS is described as follows:

$$M = M_s[1 - A/H^2] + \chi H \quad (1)$$

$$A = \frac{4K^2}{15M_s^2} \quad (2)$$

where M_s is the spontaneous magnetization. K is the magnetocrystalline anisotropy parameter. χ is the high-field susceptibility.

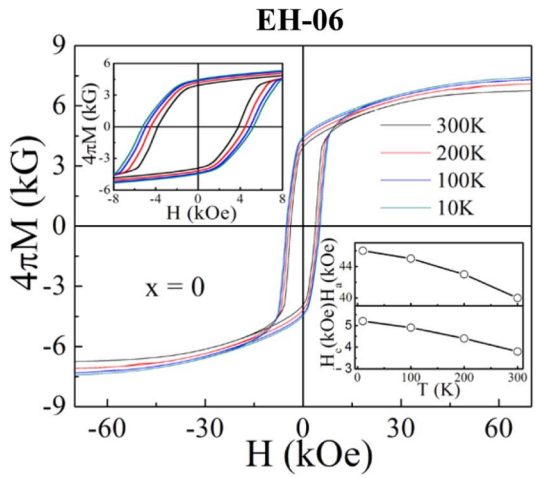

Fig. 3. Hysteresis loops at various temperature of nanocrystalline $Zr_{16}Co_{78-x}Mo_xSi_3B_3$ (x = 0). The upper left inset showing the enlarged part of hysteresis loops. The lower right inset showing temperature dependence of magnetocrystalline anisotropy parameter, anisotropy field, and coercive force.

The values of K and M_s were determined by fitting the experimental curves to (1), (2). The results are shown in Fig. 2(b). The anisotropy field was calculated as $H_a = 2K/M_s$ [10]. The saturation field of the typical sample is shown in the inset of Fig. 2(a). The saturation field of all the samples is almost the same as respective anisotropy field. It is assumed that the saturation field of the sample represents the anisotropy field of Zr_2Co_{11}. The anisotropy field of Zr_2Co_{11} is almost unchanged with x. The addition of Si and B obviously inhibits the formation of Co which may provide the nucleation site of reversed domains. Thus the coercive force of $Zr_{16}Co_{78}Si_3B_3$ increases 2.8 times in comparison with that of $Zr_{16}Co_{84}$. Mo addition together with Si and B further restrains the generation of Co. This leads to a continuous enhancement of coercive force with the increase of Mo content. For x ≥ 4, the sample consists of single Zr_2Co_{11} hard magnetic phase. The coercive force improvement with increasing Mo content may reflect the transition from random-anisotropy averaging to strong pinning as the Zr_2Co_{11} grain size increases.

Fig. 3 shows the temperature dependence of hysteresis loops for nanocrystalline $Zr_{16}Co_{78-x}Mo_xSi_3B_3$ (x = 0). The hysteresis loop at 300 K of the sample exhibits a single-phase magnetic behavior, indicating the existence of strong intergrain exchange coupling action. The coercive force of the sample enhances with the reduction of the temperature. This results from the increase of the anisotropy field for Zr_2Co_{11}. Generally, intergrain exchange coupling (IEC) is positively proportional to $(A/K)^{1/2}$ [11], where, A is the exchange constant of soft magnetic phase, and K is the magnetocrystalline anisotropy parameter of hard magnetic phase. The lower right inset shows that K of Zr_2Co_{11} has a small change with the reduction of temperature. It is inferred that IEC slightly changes with the decrease of temperature. Thus, the rectangular shape of demagnetization curves for x = 0 is almost unchanged with the reduction of temperature.

Fig. 4 shows wheel speed dependence of the coercive force for nanocrystalline $Zr_{16}Co_{78-x}Mo_xSi_3B_3$ (x = 4).

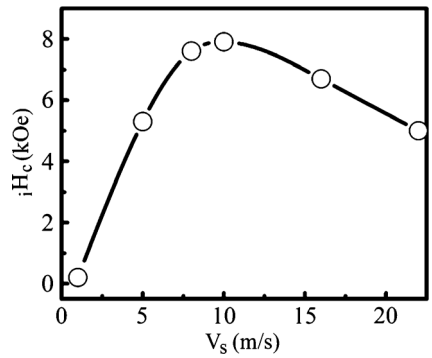

Fig. 4. Wheel speed dependence of coercive force for nanocrystalline $Zr_{16}Co_{78-x}Mo_xSi_3B_3$ (x = 4).

The coercive force of the sample has a maximum coercive force at a critical wheel speed of almost 10 m/s. As wheel speed is smaller than this value, the crystallite becomes larger. Coercive force decreases because the grain subdivides into multidomains. When wheel speed is larger than the critical value, the crystallite becomes smaller and the coercive force decreases. Coercive force also decreases because intergrain exchange coupling action strengthens and the effective anisotropy weakens. This kind of grain size dependence of coercive force may be a character of single-phase permanent magnetic materials. Similar phenomenon was observed in single-phase $Sm(Co, Fe, Cu, Zr)_7$ nanocrystalline materials [12].

IV. Conclusion

The Zr_2Co_{11}-based nanocrystalline materials have been produced by melt spinning. Structure and magnetism of nanocrystalline $Zr_{16}Co_{78-x}Mo_xSi_3B_3$ (x = 0, 2, 3, 4, 5) has been investigated. The samples are composed of rhombohedral Zr_2Co_{11} and hcp Co, where Zr_2Co_{11} is the hard phase. Its crystal structure is rhombohedral. Mo addition strongly inhibits the formation of Co which usually is the nucleation center of reversed domain. Therefore, coericive of the specimen was greatly enhanced. A coercive force of 7.9 kOe, which is 7 times higher than that of alnico, was obtained for $x = 5$. The saturation field of the sample may represent the anisotropy field of Zr_2Co_{11}. The coercive force enhancement of $x = 0$ with the reduction of temperature arises from the increase of anisotropy field. The magnetization of the Zr_2Co_{11} nanocrystalline materials with single phase may be improved by adding limited amounts of Fe or introducing soft magnetic phase Co with a small cost of coercive force.

Acknowledgment

This work is supported by DOE/Ames/BREM under grant DE-AC02-07CH11358.

References

[1] R. Kuentzler, A. Amamou, R. Clad, and P. Turek, "Electronic structure, superconductivity and magnetism in the Zr-Co system," *J. Phys. F: Met. Phys.*, vol. 17, pp. 459–474, Feb. 1987.

[2] D. Okai, R. Nagai, G. Motoyama, T. Fukami, T. Yamasaki, Y. Yokoyama, H. M. Kimura, and A. Inoue, "Superconducting property of Zr-Co and Zr-Co-Al alloys fabricated by rapid solidification," *Physica C*, vol. 470, pp. 1048–1051, Nov. 2010.

[3] A. M. Ghemawat, M. Foldeaki, R. A. Dunlap, and R. C. O'Handley, "New microcrystalline hard magnets in a Co-Zr-B alloy system," *IEEE Trans. Magn.*, vol. 25, no. 5, pp. 3312–3314, Sep. 1989.

[4] T. Ishikawa and K. Ohmori, "Hard magnetic phase in rapidly quenched Zr-Co-B alloys," *IEEE Trans. Magn.*, vol. 26, no. 5, pp. 1370–1372, Sep. 1990.

[5] G. V. Ivanova, N. N. Shchegoleva, and A. M. Gabay, "Crystal structure of Zr2Co11 hard magnetic compound," *J. Alloys Compd.*, vol. 423, pp. 135–141, Apr. 2007.

[6] E. Burzo, R. Grössinger, P. Hundegger, H. R. Kirchmayr, R. Krewenka, O. Mayerhofer, and R. Lemaire, "Magnetic properties of $ZrCo_{5.1-x}Fe_x$ alloys," *J. Appl. Phys.*, vol. 70, pp. 6550–6552, Nov. 1991.

[7] G. Stroink, Z. M. Stadnik, G. Viau, and R. A. Dunlap, "The influence of quenching rate on the magnetic properties of microcrystalline alloys $Co_{80}Zr_{20-x}B_x$," *J. Appl. Phys.*, vol. 67, pp. 4963–4965, May 1990.

[8] J. B. Zhang, Q. W. Sun, W. Q. Wang, and F. Su, "Effects of Mo additive on structure and magnetic properties of $Co_{82}Zr_{18}$ alloy," *J. Alloys Compd.*, vol. 474, pp. 48–51, Apr. 2009.

[9] G. C. Hadjipanayis, D. J. Sellmyer, and B. Brant, "Rare-earth-rich metallic glasses. I. Magnetic hysteresis," *Phys. Rev. B*, vol. 23, pp. 3349–3354, Apr. 1981.

[10] D. J. Sellmyer, Y. F. Xu, M. L. Yan, Y. C. Sui, J. Zhou, and R. Skomski, "Assembly of high-anisotropy $L1_0$ FePt nanocomposite films," *J. Magn. Magn. Mater.*, vol. 303, pp. 302–308, Aug. 2006.

[11] T. Zhao, Q. F. Xiao, Z. D. Zhang, M. Dahlgren, R. Grössinger, K. H. J. Buschow, and F. R. de Boer, "Effect of magnetocrystalline anisotropy on the magnetic properties of Fe-rich R-Fe-B nanocomposite magnets," *Appl. Phys. Lett.*, vol. 75, pp. 2298–2300, Oct. 1999.

[12] R. J. Joseyphus, A. Narayanasamy, R. Gopalan, V. Chandrasekaran, B. Jeyadevan, and K. Tohji, "Magnetic properties of mechanically milled Sm-Co permanent magnetic materials with the $TbCu_7$ structure," *Mater. Trans.*, vol. 47, pp. 2264–2268, Sep. 2006.